BioSim

Dillon Nys

April 2019

Contents

Part I
Introduction

1 Motivation

Figure 1: Falcon 9

As we enter a new era of pushing the boundaries of space exploration back to the moon and beyond to Mars, so too must there be an effort to reevaluate our preparedness in developing and maintaining habitats which can support humans on these distant rocks. Much of the information about these enclosures has come from NASA research in the 70s and 80s, and independent projects like the Biosphere (early 1990s). The conclusion of all of these studies is that there is a lot to be understood when it comes to the complex system of recycling and regeneration which is required when resources, namely water and oxygen, are scarce and must be replenished from Earth. This project opens the door to further work in the area of simulation and modeling of these environments, tools which will be crucial in both feasibility and cost estimation studies in the coming decades.

2 Background

2.1 Closed-Loop Systems

A closed-loop system is a system in which all material components after initial closure are produced, consumed, and recycled within the system, such as the water cycle (Figure 2).

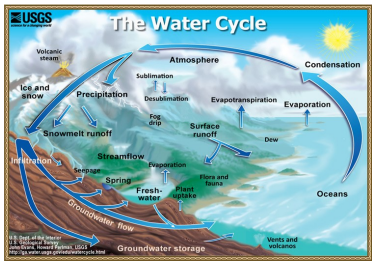

Figure 2: The water cycle

One of the earliest designs intended to replicate Earth's natural regenerative systems (collectively called the biosphere) was Bios-3, a Russian experiment in regenerative feedback systems. At a cost of $1 million in 1972, Bios-3 was the third generation in a series of increasingly complex demonstrations of materially closed-loop systems which used the natural processes of plants and algae to recycle carbon dioxide and provide nutrition for humans inside [27].

The difficulty in designing such a system is that it requires understanding every environmental factor—biological, chemical, and ecological—through and through, and in a number of different configurations. Broadly, though, it is

easy to envision what some of those components would be: O2, CO2, and trace gas levels and the associated chemical breakdown and respiration pathways, plant growth and interrelations with other communal species, human respiration and metabolism and requirements for food, water, and air quality, and the construction process for a fully-sealed environment. Ensuring that the crew operating the station are trained in all relevant processes, emergency procedures, and team dynamics is a part of the system which, though easy to ignore, should not be taken for granted.

2.2 NASA (1970s-Today)

For researchers at NASA's Ames Center, the summer of 1977 was an exciting time. A six-week long study was hosted covering a range of interests in Space Exploration and Human Settlements, which was at the time the "largest and most comprehensive investigation of space manufacturing and habitation," covering topics in regenerative life-support systems, studies of efficient habitats in space, detection of asteroids for material collection, EM mass drivers for interorbital engines, and chemical processing of nonterrestrial material in space [3].

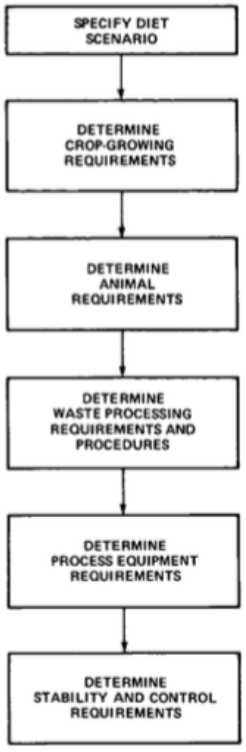

Figure 3: CELSS food system design

In their review of regenerative life-support systems—of particular interest to the engineers a closed-loop habitat—they conclude that, in the long-term, a fully regenerative design should be implemented in order to maximize economic efficiency [3]. Recognizing this, the researchers then outline a vision for investigating, evaluating and developing the technical components necessary for such systems. In their report, they discuss the limitations of the knowledge of the time including the nutritional requirements for humans not being fully understood; the lack of expertise as to how to rely on plants for reliable production of food, instead of consuming prepared foods; the uncertainty of containing and tracing environmental contaminants; the added complexity of integrating animals into the system; the handling of human waste and other organic scraps; and the risk of microbiological and other environmental hazards [3]. For each of the systems, they outline initial ideas for research, as well as develop some specific frameworks around the systems such as the agricultural development model in Figure 3.

Throughout the 1980s and 90s, NASA made serious headway in investigating these phenomena with the Controlled Ecological Life Support System (CELSS) Program established as a result of the Ames study [26, 32]. The results of this decade-long pro-

gram solidified groundwork for agricultural, human waste, and systems management investigations in the context of CELSS. One project, the Kennedy Space Center Breadboard project, set an original goal to "design, construct and test a ground-based CELSS at a one-person scale" [16]. This later evolved to "[evaluating] long-term operation of the biomass production system with increasing material closure" [11]. By the end of the 1990s, there had been no actual experiment by NASA which studied humans in a fully closed-loop environment.

The work of the CELSS division would also be the last major program to look into closed systems, as funding slowly dwindled throughout the 90s. Though thanks to the construction of the ISS and the several manned space missions throughout the 2000s, there was a revamped effort to investigate the physiological effects of humans in space with the founding of the Human Research Program (HRP).

Founded in 2005, the HRP's goal is to "provide human health and performance countermeasures, knowledge, technologies, and tools to enable safe, reliable, and productive human space exploration" [22] (Figure 4). A number of "evidence reports" have been produced because of the program, which summarize and evaluate relevant bodies of research based on a critical 4-level metric of evidence credibility, ranging from Level I ("expert committee reports or opinions of respected authorities") to Level IV ("at least one randomized, controlled trial") [22]. They are independently verified yearly by the Institute of Medicine's Committee on NASA's Research [20].

One such evidence report, entitled "Risk of Inadequate Nutrition," catalogs in great detail the broad range of micronutrients which support human health, and the experimental knowledge acquired from both ground-based and space missions [30]. This is a major success for closed-loop systems design, and the initial step in Spurlock and Modell's agricultural design framework (Figure 3). Along with the work from the CELSS Program, it's clear we have made some advancements in the Ames study objectives. Though there is still much to understand.

Figure 4: Human Research Program

Most recently, NASA has been focusing on the social dynamics of sending teams into space, specifically under the notion that the researchers who sign themselves up to the journey will likely be making a one-way trip and thus be isolated from civilization once they arrive, confined to their small living space, a so-called "isolated, confined, and extreme (ICE)" environment. Even with all environmental, nutritional, and agricultural systems and control measures in place and understood among the community, there is still the potential that not everyone will remain content and that, as time progresses, there will be new and perhaps negative behavioral and psychological factors among team members.

Figure 5: NASA HI-SEAS

NASA's ongoing missions at an isolated dome in the Hawaiian desert (Figure 5), collectively named HI-SEAS, are providing some interesting data into the psychological and physiological effects of how to maintain cooperation and wellbeing in these ICE environments [4]. In their experiments, crew members are subjected to a simulated Mars environment, where they cannot leave their small enclosed habitat. One study by Dr. Peter Roma is investigating a novel system he calls COHESION, a computer game which systematically creates team-based tasks requiring interdependence and measures cooperation and other social factors [6]. Initial data suggests such a system can reduce stress, increase positive feelings, and facilitate achievement in teams [4]. Another team led by Dr. Steve Kozlowski is hoping to gather critical data in regard to measuring physiological factors of long-term isolation as well as develop protocols for supporting teams in these environments. Both of theirs's research will be published after the current round of HI-SEAS missions. And given the amount of uncertainty which remains in this relatively new field of study, this is surely a topic whose developments should be closely followed.

2.3 Biosphere 2 (1980s-90s)

In recognizing that Earth itself is a materially closed-loop and self-sustaining system, a team of researchers in the late-80s set out to design a scaled-down version of this biosphere, which they named affectionately Biosphere 2 (Figure 6). The goal was to replicate the different biomes of Earth under one enclosed structure, sealed from the outside world and able to support human life solely with the local constructed environment [17]. This included growing food, providing a constant supply of freshwater, and controlling climatic variables and atmospheric gas concentrations. All the while, they were to record and measure levels of environmental variables and monitor the health of the researchers with on-site doctors [8].

Figure 6: Biosphere 2

Biosphere 2's design was unique for a number of reasons. Because of its

level of complexity and fully enclosed nature (which had never been built on its scale before), there were a number of engineering challenges which needed to be tackled [17]. One of the bigger challenges was due to the pressure differences which would arise with changing indoor humidity levels. In order to combat this, the engineers installed a system of two artificial lungs—large offsite chambers which could expand and deflate as needed. And then there was the matter of creating an airtight seal. To accomplish this, a number of high-grade stainless steel panels were welded together and used to line the concrete foundation. These, along with a 12mm silicone-caulked gap and sophisticated leak detection systems, helped to ensure an airtight seal for the entire structure [36]. In the end, the engineers achieved a leak rate of only 10% per year [9].

The majority of the research here came out of the two periods when researchers were sealed inside—the first, called Mission One, took place from 1991 to 1993 for a period of two years, and the second, Mission Two, was completed in 1994 for a period of 6 months [1]. What came from this is an abundance of information in regard to material flows, or tracing the lifecycle of several of the organic and non-organic compounds in the system. After all, every atom which was there at the beginning was there in some form at the end (more or less)—the underlying beauty and necessity of studying in a closed-loop environment.

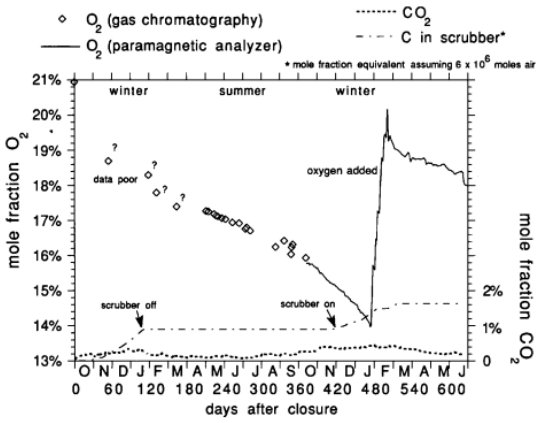

Figure 7: Biosphere 2 O_2 levels

Oxygen levels were of particular concern as they declined steadily in the first 16 months of enclosure (Figure 7). The problem seemed to be that the concrete was absorbing a significant portion of atmospheric CO2, offsetting the respiration-photosynthesis balance of soil microbes and plants, which should naturally be synchronized [29].

Food was also a difficult system to control. And while the Biosphere's creators designed the system to support a diet of 2500 kcal for each of the 8 crew members of Mission One, the average caloric intake in the first 6 months measured only ∼1780, rising to ∼2000 in the remaining time, leading to significant physiological changes including weight loss, decreased hormones, and decreased biochemical indicators such as cholesterol, blood sugar, and blood pressure. Dr. Roy Walford—who was a member of the Mission One crew and the supervising medical doctor—and his colleagues declared that despite all this, the crew members remained in "excellent" physical health [21].

The problem with the agriculture was that there were unexpectedly low light levels in the growing area due to the structural frame and double laminated

glass which filtered away nearly 50% of available sunlight [7]. The use of soils with high organic content led the soil to become highly saline over time and created extra problems with regards to plant biomass in the form of compost, which could not be easily reintegrated [18]. And the decision to not use toxic pesticides ultimately caused further productivity decreases as crops suffered from increased pest damage and fungal disease [18].

Despite the many problems of Mission One, though, it did provide some positive insights as well. The fully functional constructed wetland which processed 240-290 gal/day of human effluent and supported 14 unique wetland species [23]. Mission Two delivered expectedly better results with better agriculture yields and health and fewer issues overall due to a better understanding of the systems and learning from the mistakes of Mission One. In fact, the agricultural yields of Mission Two rose to higher than agrarian yields in Indonesia, Southern China, and Bangladesh, according to researchers [18].

Overall, although the design of Biosphere 2 would seem to be based in conflicting agendas of establishing regenerative life support systems and modeling the many biomes of Earth, the experiment ultimately resulted in a breadth of research and began preliminary testing of human coupling with their environment in CELSS—a claim which only Russia's Bios-3 can match as of right now.

Part II
Model

3 Heat Transfer

Equations related to the transfer of heat.

$$Q = mc\Delta T \tag{3.1}$$
$$Q = mL \tag{3.2}$$

3.1 Assumptions

Assumptions for this section are:

- Complete mixing of fluids within the model Δt step (1 hour)
- Thermodynamic equilibrium is reached within the model Δt step

3.2 Water

Heat transfer at the water surface. J represents the total heat flux in W/m^2. Incoming radiation at the surface is divided into short-wave (J_{sn}) and long-wave (J_{an}) where short-wave radiation comes from the lights used to light the BioSim and long-wave radiation comes from the atmosphere itself.

The total heat flux can be represented by the following equation [5]:

$$J = J_{sn} + J_{an} - (J_{br} + J_c + J_e) \tag{3.3}$$

where

J = The total heat flux (W/m^2)
J_{sn} = Short-wave radiation flux (W/m^2)
J_{an} = Long-wave radiation flux (W/m^2)
J_{br} = Black-body radiation flux (W/m^2)
J_c = Convection-conduction radiation flux (W/m^2)
J_e = Evaporation-condensation radiation flux (W/m^2)

3.2.1 Short-wave radiation (J_{sn})

Short-wave radiation will be supplied to the water through overhead LED lights. Different lights will be available for growing and living spaces, each with a different light spectrum, energy requirement, and heat output.

To calculate short-wave radiation:

$$J_{sn} = \frac{N_{\text{bulbs}} H_{\text{bulb}}}{A} \tag{3.4}$$

where

J_{sn} = Short-wave radiation flux (W/m^2)
N_{bulbs} = The number of light bulbs
H_{bulb} = The heat per light bulb (W)
A = Area of lit space (m^2)

3.2.2 Long-wave radiation (J_{an})

Long-wave radiation is caused by the absorption, emission, and scattering of infrared radiation by the atmosphere.

It can be calculated using the following equation [5]:

$$J_{an} = \sigma(T_{\text{air}} + 273.15)^4(A + 0.031\sqrt{e_{\text{air}}/0.13332})(1 - R_L) \tag{3.5}$$

where

J_{an} = Long-wave atmospheric radiation flux (W/m^2)
σ = Stefan-Boltzmann constant (5.67×10^{-8} W m^{-2} K^{-4})
T_{air} = Air temperature (°C)
A = A coefficient (0.5 to 0.7)
e_{air} = Air vapor pressure (kPa)
R_L = Reflection coefficient (≈ 0.03)

3.2.3 Black-body radiation (J_{br})

Black-body radiation is the long-wave radiation emitted from all objects. It is emitted from the water body and is responsible for the first term in the loss side of the total heat flux equation.

It can be calculated using the following equation [5]:

$$J_{br} = \epsilon\sigma(T_s + 273.15)^4 \tag{3.6}$$

where

J_{br} = Black-body radiation flux (W/m^2)
ϵ = Emissivity of water (≈ 0.97)
σ = Stefan-Boltzmann constant (5.67×10^{-8} W m^{-2} K^{-4})
T_s = Water surface temperature (°C)

3.2.4 Conduction/Convection (J_c)

Conduction and convection both contribute to the total heat flux at the surface of the water.

When air flows over water and the water surface is warmer than the air, convection can be calculated using the following equations [5]:

$$J_c = h_c(T_s - T_{\text{air}}) \tag{3.7}$$

$$h_c = 10.45 - u + 10\sqrt{u} \tag{3.8}$$

where

J_c = Conduction-convection heat flux (W/m^2)
h_c = Convective heat transfer coefficient (W m^{-2} K^{-1})
u = Wind velocity at the surface (m/s)

However, when the air which flows over the surface is cooler and the water and the heat exchange direction is reversed, the convective heat transfer coefficient h_c must be estimated using the Nusselt number [2]:

$$\text{Nu} = \frac{h_c L}{k} = \left(0.037\text{Re}^{4/5} - 871\right)\text{Pr}^{1/3} \tag{3.9}$$

$$\text{Re} = \frac{\rho u L}{\mu} \tag{3.10}$$

$$\text{Pr} = \frac{\mu C_p}{k} \tag{3.11}$$

where

h_c = Convective heat transfer coeff. from air $\rightarrow$ water (W m^{-2} K^{-1})
L = Characteristic length of water surface (m)
k = Thermal conductivity of water (m)
ρ = Density of water (kg/m^3)
μ = Dynamic viscosity of water (kg/m^3)
C_p = Water isobaric heat capacity (J kg^{-1} K^{-1})
Nu = Nusselt number (unitless)
Re = Reynolds number (unitless)
Pr = Prandtl number (unitless)

3.2.5 Evaporation (J_e)

In order to calculate the heat transfer due to evaporation, the total mass of evaporated water is first calculated.

$$m_e = (x_s - x)a_e \tag{3.12}$$

$$a_e = \frac{25 + 19u}{3600} \tag{3.13}$$

where

m_e = Mass flux of water evaporated (kg m^{-2} s^{-1})
x = Actual humidity ratio (kg/kg)
x_s = Saturation humidity ratio (kg/kg)
a_e = Evaporation coefficient (kg m^{-2} s^{-1})
u = Wind velocity at water surface (m/s)

Then the total heat transfer can be calculated using the heat transfer formula (6.3):

$$J_e = m_e L \tag{3.14}$$

and by estimating the latent heat of evaporation of water (6.3).

J_e = Evaporative heat flux (W/m^2)
m_e = Mass flux of evaporated water (kg m^{-2} s^{-1})
L = Latent heat of evaporation (J/kg)

3.2.6 Condensation (J_d)

Condensation is a function of the temperature relative to the dew point. Thus, condensation only occurs if it is forced (i.e. through the use of a dehumidifier) or if the temperature drops below the dew point. The heat transfer due to dew forming can be calculated using the equation for heat transfer (6.3):

$$J_d = m_d L \tag{3.15}$$

where

J_d = Condensation heat flux (W/m^2)
m_d = Mass flux of dew deposited (kg m^{-2} s^{-1})
L = Latent heat of evaporation (J/kg)

4 Crop Growth

Equations related to crop growth modeling. Most equations, unless otherwise noted, are derived from [28].

4.1 Background

These equations are based off the RI-RUE model developed by Monteith.

$$RG_t = RUE_t \times RAD_t \times (1 - \exp[-k \times LAI_t]) \tag{4.1}$$

$$DBM = \int_0^t RG_t \times dt \tag{4.2}$$

where

RG = Rate of plant growth (g)
RUE = Radiation use efficiency (g/MJ)
RAD = Radiation (MJ)
k = Radiation extinction constant [1]
LAI = Leaf area index (m^2/m^2)
DBM = Dry biomass (g)

Leaf area index is calculated as a function of the specific leaf area (SLA), which is itself a function of the development stage of the crop (DVS), and the leaf biomass at time t ($LeafB_t$).

$$LAI_t = SLA_t \times LeafB_t \tag{4.3}$$

where

SLA = Specific leaf area (m^2/g)
$LeafB$ = Leaf biomass per unit area (g/m^2)

4.2 Assumptions

- Many constants and parameters are assumed based off a specific crop in specific conditions (see "Interpolated Values")
- Crop parameters are constant throughout all crop cycles

4.3 Procedure

To begin, the development stage (DVS) is calculated using the following relationship (Fig. 8):

[1] As explained in [25], radiation will be intercepted at different rates depending on the structure (size and shape) of the leaf canopy. For erect, horizontal leaves, this value ranges from 0.6 to 0.8.

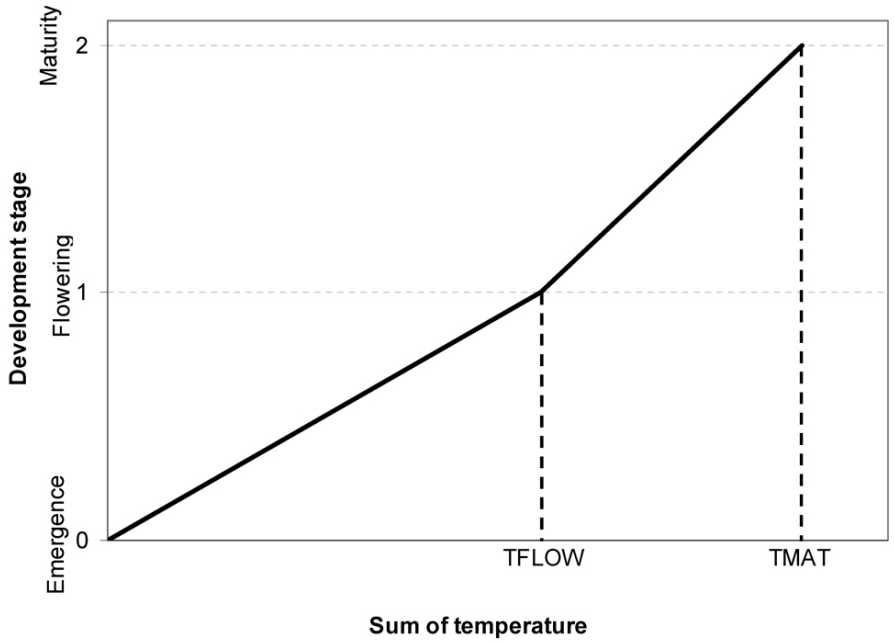

Figure 8: Plot of GDD (i.e. Sum of temperature) vs. DVS [28]

$$DVS_t = \begin{cases} GDD_t/GDD_{flow}, & \text{if } GDD_t < GDD_{flow} \\ 1 + (GDD_t - GDD_{flow})/(GDD_{mat} - GDD_{flow}), & \text{if } GDD_t \geq GDD_{flow} \end{cases} \tag{4.4}$$

where

GDD_t = Growing degree days at time t (°C-day)
GDD_{flow} = Growing degree days at flowering (°C-day)
GDD_{mat} = Growing degree days at maturity (°C-day)

The flowering and maturity GDDs are unique to each crop and have been acquired for wheat, soy, and corn from various sources. To calculate the growing degree days for a crop (GDD), the following equation is used.

$$GDD_t = \int_0^t [\min(T_{air}, T_{max}) - T_{base}]\, dt \tag{4.5}$$

where

T_{air} = Mean air temperature (°C)
T_{max} = Cutoff temperature beyond which crop does not benefit (°C)
T_{base} = Cutoff temperature below which crop does not benefit (°C)

Values for T_{max} and T_{base} are available in various sources for wheat, corn, and soy, and for the purposes of this simulation, the trapezoid method was used to estimate the above integral.

A step-wise process is then taken involving the partitioning of total available photosynthetic energy ($POOL$) into the leaves ($LeafB$), stems ($StemB$), roots ($RootB$), and storage organs ($StorB$).

$$POOL_{t+\Delta t} = POOL_t + (RG_t \times \Delta t) \tag{4.6}$$

$$LeafB_{t+\Delta t} = LeafB_t + (PartL_t \times \Delta t) \tag{4.7}$$
$$StemB_{t+\Delta t} = StemB_t + (PartS_t \times \Delta t) \tag{4.8}$$
$$RootB_{t+\Delta t} = RootB_t + (PartR_t \times \Delta t) \tag{4.9}$$
$$StorB_{t+\Delta t} = StorB_t + (PartSO_t \times \Delta t) \tag{4.10}$$

where $PartL$, $PartS$, $PartR$, and $PartSO$ are the daily flows of biomass to the leaves, stems, roots, and storage organs, respectively. To calculate these:

$$PartL_t = POOL_t \times CPL_t \times (1 - CPR_t) \tag{4.11}$$
$$PartS_t = POOL_t \times CPS_t \times (1 - CPR_t) \tag{4.12}$$
$$PartR_t = POOL_t \times CPR_t \tag{4.13}$$
$$PartSO_t = POOL_t \times CPSO_t \times (1 - CPR_t) \tag{4.14}$$

where CPL, CPS, CPR, and $CPSO$ are the partitioning coefficients for the leaves, stems, roots, and storage organs, which depend on the development stage (DVS). Values for these are fixed and interpolated for values of DVS (see "Interpolated Values").

After calculating these values, (4.6) can be transformed to incorporate partitioning of available resources.

$$POOL_{t+\Delta t} = POOL_t + (RG_t - PartL_t - PartS_t - PartR_t - PartSO_t) \times \Delta t \tag{4.15}$$

4.3.1 Leaf Senescence

Incorporating the relative rate of leaf biomass decline due to aging ($rrsenl$), the rate of leaf biomass growth (4.7) can be transformed:

$$LeafB_{t+\Delta t} = LeafB_t + (PartL_t - RSenL_t) \times \Delta t \tag{4.16}$$
$$RSenL_t = rrsenl_t \times LeafB_t \tag{4.17}$$

4.3.2 Accumulation and redistribution of reserves

In later stages of development, biomass can translocate between the stem or roots and storage organs. Thus, incorporating this factor ($RTransloc$), (4.8)

and (4.10) become:

$$StemB_{t+\Delta t} = StemB_t + (PartS_t - RTransloc_t) \times \Delta t \tag{4.18}$$

$$StorB_{t+\Delta t} = StorB_t + (PartSO_t - RTransolc_t) \times \Delta t \tag{4.19}$$

$$RTransloc_t = \begin{Bmatrix} 0 & DVS \leq 1 \\ 0.005 \times MaxStemB & DVS > 1 \end{Bmatrix} \tag{4.20}$$

$$MaxStemB_{t+\Delta t} = MaxStemB_t + PartLS \tag{4.21}$$

$$PartLS = PartL + PartS \tag{4.22}$$

4.4 Evapotranspiration

Evapotranspiration (ET_0) is calculated using the Penman-Monteith equation, following the procedure of [37]. The so-called FAO 56 Penman-Monteith equation is a standardized method of calculating reference evapotranspiration for "a hypothetical reference crop with crop height of 0.12 m, a fixed surface resistance of 70 s m^{-1} and an albedo value[...] of 0.23." It takes the form below[2]:

$$ET_0 = \frac{0.408(R_n - G) + \gamma \frac{37.5}{T+273} u_2 (e_s - e_a)}{\Delta + \gamma(1 + 0.34u_2)} \tag{4.23}$$

where

ET_0 = Reference evapotranspiration (mm hr^{-1})
R_n = Net radiation at the crop surface (MJ m^{-2} $hr^{=1}$)
G = Soil heat flux density (MJ m^{-2} $hr^{=1}$)
T = Mean hourly air temperature at 2 m height (°C)
u_2 = Wind speed at 2 m height (m s^{-1})
e_s = Saturation vapor pressure (kPa)
e_a = Actual vapor pressure (kPa)
Δ = Slope of saturation vapor pressure curve (kPa $°C^{-1}$)
γ = Psychometric constant (kPa $°C^{-1}$)

Crop-specific ET is then computed using the equation

$$ET_c = K_c \times ET_0 \tag{4.24}$$

where K_c is the crop coefficient. Values for K_c can be approximated using the regression equations of [24]. The equations for wheat, soy, and corn are shown below.

$$\textbf{Wheat: } K_c = 2.7 \times 10^{-1} - 4.8 \times 10^{-4} GDD_t + 6.27 \times 10^{-7} GDD_t^2 - 1.3 \times 10^{-10} GDD_t^3 \tag{4.25}$$

[2]For a daily time step, the numerator constant 37.5 is multiplied by 24

Corn: $K_c = 1.2 \times 10^{-1} + 1.68 \times 10^{-3} GDD_t -$
$$2.46 \times 10^{-7} GDD_t^2 - 4.37 \times 10^{-10} GDD_t^3 \quad (4.26)$$

Soy: $K_c = 4.35 \times 10^{-2} + 1.37 \times 10^{-3} GDD_t -$
$$5.3 \times 10^{-7} GDD_t^2 - 5.43 \times 10^{-11} GDD_t^3 \quad (4.27)$$

4.5 Interpolated Values

The following values are used in the crop growth equations. They are based on a model for rice production in South Asia [35, 28].

DVS	CPR	CPPL	CPPP	rrsenl	SLA
0	0.3	0.55	0	0	0.037
0.05			0		
0.1	0.263	0.536	0	0	
0.15			0		
0.2	0.225	0.521	0	0	
0.25			0		
0.3	0.188	0.507	0	0	
0.35			0		
0.4	0.15	0.493	0	0	
0.45			0		
0.5	0.112	0.479	0	0	
0.55			0		
0.6	0.075	0.464	0	0	
0.65			0		
0.7	0.038	0.45	0	0	
0.75			0		
0.8	0	0.3	0.143	0	
0.85			0.286		
0.9	0	0.15	0.429	0	
0.95			0.571		
1	0	0	0.714	0	0.018
1.05			0.857		
1.1	0	0	1	0.013	
1.15			1		
1.2	0	0	1	0.026	
1.25			1		
1.3	0	0	1	0.04	
1.35			1		
1.4	0	0	1	0.04	
1.45			1		
1.5	0	0	1	0.04	
1.55			1		
1.6	0	0	1	0.04	
1.65			1		
1.7	0	0	1	0.04	
1.75			1		
1.8	0	0	1	0.04	
1.85			1		
1.9	0	0	1	0.04	
1.95			1		
2	0	0	1	0.04	0.017

5 Water Treatment

The following treatment train was chosen for regenerating water from human waste streams.

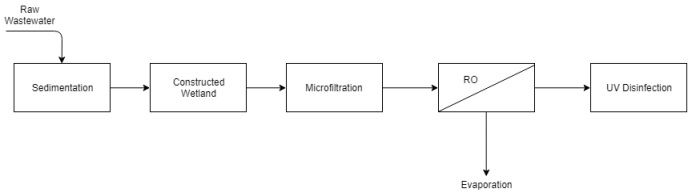

Figure 9: Wastewater treatment train

5.1 Sedimentation

To model the sedimentation of particles in the pre-treatment basin, a simple set of equations is used [12]. To model the settling velocity of particles:

$$v_s = \frac{g(\rho_p - \rho_w)d_p^2}{18\mu} \qquad \text{Re} < 2 \ \text{ (laminar flow)} \tag{5.1}$$

$$v_s = \left[\frac{g(\rho_p - \rho_w)d_p^{1.6}}{13.9\rho_w^{0.4}\mu^{0.6}}\right]^{1/1.4} \qquad 2 \leq \text{Re} \leq 500 \ \text{ (transition flow)} \tag{5.2}$$

where

$$\text{Re} = \frac{\rho_w v_s d_p}{\mu} = \frac{v_s d_p}{\nu} \tag{5.3}$$

and

v_s = Settling velocity of the particle (m/s)
g = Acceleration due to gravity, 9.81 m/s^2
ρ_p = Density of the particle (kg/m^3)
ρ_w = Density of water (kg/m^3)
C_d = Drag coefficient, unitless
d_p = Diameter of particle (m)
Re = Reynolds number, dimensionless
μ = Dynamic viscosity (N·s/m^2)
ν = Kinematic viscosity (m^2/s)

Based off the particle velocity and properties of the water, the sedimentation basin dimensions can be calculated so that all particles with a diameter greater than D (i.e. $d_p \geq D$) will be fully removed. To do so, the following equation is used:

$$v_D = v_c = \frac{h_0}{\tau} = \frac{h_0 Q}{h_0 A} = \frac{Q}{A} \implies A = \frac{Q}{v_D} \tag{5.4}$$

where

v_D = Settling velocity of particle with diameter D (m/s)
v_c = Critical velocity such that particle at surface of inlet is removed just before outlet (m/s)
h_0 = Height of the sedimentation basin (m)
τ = Hydraulic retention time in basin (s)
Q = Sedimentation basin loading rate (m^3/s)
A = Sedimentation basin area (m^2)

Once the area is calculated, the length, width, and depth can be determined using a preferential L:W ratio of 5:1 and a preferential depth of 4 m [12].

The fraction of particles removed for a specific diameter less than D, the following equation can be used:

$$\text{Fraction of particles removed} = \frac{v_s}{v_D} \, (v_s < v_D) \tag{5.5}$$

5.2 Wetlands Treatment

5.2.1 Green-Ampt Modeling

The Green-Ampt equation [15] is used to model infiltration into a vertical constructed wetland. For a one-layer wetland, the following equation is used to calculate the time to saturate the wetland with or without ponding at the surface[3].

$$t_1 = \frac{\theta_s - \theta_i}{K_s} \left[z_1 - \Delta h \ln \left(1 + \frac{z_1}{\Delta h} \right) \right] \tag{5.6}$$

$$\Delta h = h_0 - \Psi_f \tag{5.7}$$

$$\theta_i \approx \theta_{fc} = \phi \left(\frac{|\Psi_{ae}|}{340} \right)^{\frac{1}{b}} \tag{5.8}$$

$$|\Psi_f| \approx \frac{|\Psi_{ae}|}{2} \tag{5.9}$$

where

t_1 = Time to saturate one-layer wetland (hr)
θ_s = Saturated water content (= to porosity ϕ)
θ_i = Initial water content[4]
θ_{fc} = Soil field capacity, i.e. the water content held against gravity[5]
K_s = Saturated hydraulic conductivity (m hr^{-1})
z_1 = Depth of the wetland basin (m)
Δh = Pressure head difference (m)
Ψ_f = Suction head of the wetting front (m)[6]
ϕ = Porosity of the material

[3]Note: For consistency, $\Psi < 0$ and $h_0 \geq 0$. Thus, Δh will always be ≥ 0.
[4]Equation for soil field capacity is used to represent a "dry" soil after first wetting. θ_i can be set to 0 for first wetting.
[5]Derived from [10].
[6]This approximation is established in [15].

5.3 Treatment Kinetics

Kinetics are modeled using the $P-k-C*$ model of [14] with areal rate constants derived from [19]:

$$\frac{C - C^*}{C_i - C^*} = \left(1 + \frac{k_A y}{Pq}\right)^{-P} \tag{5.10}$$

where

C = Concentration at y (mg/L)
C_i = Concentration at inlet (mg/L)
C^* = Background concentration (mg/L)
k_A = Areal rate constant (m/day)
y = Depth in wetland (m)
P = apparent number of TIS[7]

Values for k_A are summarized below (Table 1) for a wetland packed with 0-4 mm gravel ($d_{10} = 0.55$mm, $d_{60} = 3.1$mm) and planted with common reed plants (*Phragmites australis*).

Pollutant	k_A **(m/day)**
BOD_5	0.43
TSS	0.28
NH_4^+	0.56

Table 1: k_A rate constants from [19]

5.4 Filtration

5.4.1 TSS Removal

While the rate constants above can only be verified through experimentation, the rate of removal of TSS can be estimated using an independent set of equations if we consider the wetland equivalent to a rapid granular filter. This will serve to verify, perhaps, the k_A value from Table 1.

Yao et al. developed a model of water filtration based off filter media grains acting as collectors for particles which enter their region of influence. The mass removal is calculated as the rate at which particles enter their proximity multiplied by a transport efficiency (η) and attachment efficiency factor (α). The mass balance was developed by Crittenden et al. to be modeled as a first-order reaction [12].

$$\frac{dC}{dz} = \left(\frac{-3(1-\varepsilon)\eta\alpha}{2d_C}\right) C \implies \text{i.e. } C = C_0 \exp\left[\frac{-3(1-\varepsilon)\eta\alpha L}{2d_C}\right] \tag{5.11}$$

where

[7] TIS = Tanks in series. For our model, $P = 1$, i.e. a plug-flow system.

C, C_0 = Concentration of suspended solids (mg/L)
ε = Wetland bed porosity
η = Transport efficiency factor, unitless
α = Attachment efficiency factor, unitless
L = Wetland bed depth (m)
d_C = Diameter of wetland bed media (m)

The process for calculating the transport efficiency are described below. For this experiment, the attachment efficiency is assumed to be 1.0 [12].

Transport efficiency is divided into three primary influences: diffusion (η_D), accounting for the Brownian motion of particles which causes them to deviate from their flow path; sedimentation (η_G), which causes larger particles to more often deviate from their flow path due to gravitational forces; and interception (η_I), which causes particles passing within half a diameter of filter particles to be intercepted.

$$\eta = \eta_D + \eta_G + \eta_I \tag{5.12}$$

$$\eta_D = 2.4\, A_S^{1/3} N_R {-}0.081 N_V^{0.052} \mathrm{Pe}^{-0.715} \tag{5.13}$$

$$\eta_G = 0.22\, N_R^{-0.24} N_V 0.053 N_G^{1.11} \tag{5.14}$$

$$\eta_I = 0.55\, A_S N_A^{1/8} N_R^{1.675} \tag{5.15}$$

where

η_D = Transport efficiency due to diffusion, dimensionless
η_G = Transport efficiency due to gravity, dimensionless
η_I = Transport efficiency due to interception, dimensionless
A_S = Porosity parameter that accounts for the effect of adjacent media grains, dimensionless
N_R = Relative size number, dimensionless
N_V = van der Waals number, dimensionless
Pe = Peclet number, dimensionless
N_G = Gravity number, dimensionless
N_A = Attraction number accounting for attraction between collector and particle as the particle gets closer, dimensionless

The dimensionless numbers above can be calculated as follows:

$$A_S = \frac{2(1-\gamma^5)}{2-3\gamma+3\gamma^5-2\gamma^6} \tag{5.16}$$

$$N_R = \frac{d_p}{d_C} \tag{5.17}$$

$$N_V = \frac{\text{Ha}}{k_B T} \tag{5.18}$$

$$\text{Pe} = \frac{3\pi\mu d_p d_C v_F}{k_B T} \tag{5.19}$$

$$N_G = \frac{v_S}{v_F} = \frac{g(\rho_P - \rho_W)d_p^2}{18\mu v_F} \tag{5.20}$$

$$N_A = \frac{N_V}{N_R \text{Pe}} = \frac{\text{Ha}}{3\pi\mu d_p^2 v_F} \tag{5.21}$$

where

γ	$= (1-\varepsilon)^{1/3}$, dimensionless
ε	= Wetland bed porosity, dimensionless
d_p, d_C	= Particle and collector diameters (m)
Ha	= Hamaker constant, J
k_B	= Boltzmann constant, 1.381×10^{-23} J/K
T	= Absolute temperature (K)
μ	= Water dynamic viscosity (Pa-s)
v_F	= Superficial velocity of particles (m/s)[8]
v_S	= Stokes settling velocity (m/s)
g	= Gravitational constant, 9.81 m/s^2
ρ_p, ρ_W	= Density of particles and water (kg/m^3)

5.4.2 Head Loss

Clean bed head loss due to inertial and viscous forces can be estimated using the Ergun equation [12]:

$$h_L = \kappa_V \frac{(1-\varepsilon)^2}{\varepsilon^3} \frac{\mu L v_F}{\rho_W g d^2} + \kappa_I \frac{1-\varepsilon}{\varepsilon^3} \frac{L v_F^2}{g d} \tag{5.22}$$

where

[8] This is set equal to the hydraulic loading rate q in the simulation.

h_L = Head loss in clean bed (m)
κ_V, κ_I = Ergun coefficients for viscous and inertial losses, unitless
ε = Filter bed porosity
L = Filter bed length (m)
v_F = Superficial velocity of particles (m/s)[9]
μ = Water dynamic visocity (Pa-s)
ρ_W = Water density (kg/m^3)
g = Gravitational coefficient (9.81 m/s^2)
d = Diameter of bed media (m)

5.5 Assumptions

The main assumptions for the treatment wetlands are:

- The assumptions of the Green-Ampt equation including a sharp wetting front and complete saturation of the wetted area.
- The wetland behaves like an ideal plug-flow reactor.
- The wetlands are packed with 0.8m of 0-4 mm gravel and densely packed with common reed.
- Particle size distribution of raw wastewater follows that of [33] (Table 2).

Particle fraction (μm)	Prevalence in wastewater (%)
$d_p \leq 12$	26
$12 < d_p \leq 63$	27
$63 < d_p \leq 1000$	33
$d_p > 1000$	14

Table 2: Particle size distribution in raw wastewater

In reality, none of the assumptions above would likely hold true and thus, this is a heavily idealized system used to model an approximation of treatment quality and hydraulic characteristics.

[9] This is set equal to the hydraulic loading rate q in the simulation.

6 Water Properties

The following equations are used to estimate the properties of water.

6.1 Saturation vapor pressure (e_s)

$$e_s = 0.611 \exp\left[\frac{17.3\,T_{\text{air}}}{T_{\text{air}} + 237.3}\right] \tag{6.1}$$

where

e_S = Saturation vapor pressure (kPa)
T_{air} = Air temperature (°C)

6.2 Water density (ρ_w)

$$\rho_W = 999.5308 + 6.32693 \times 10^{-2} T_W - 8.523829 \times 10^{-3} T_W^2 + 6.943248 \times 10^{-5} T_W^3 - 3.3821216 \times 10^{-7} T_W^4 \tag{6.2}$$

where

ρ_W = Water density (kg/m^3)
T_W = Water temperature (°C)

6.3 Latent heat of evaporation (L)

$$L \approx 2362 \times (-6.178 \times 10^{-15}\, T_W^6 + 8.001 \times 10^{-12}\, T_W^5 + 4.930 \times 10^{-9}\, T_W^4 + 5.441 \times 10^{-7}\, T_W^3 + 4.451 \times 10^{-5}\, T_W^2 - 0.562\, T_W + 1093.2) \tag{6.3}$$

where

L = Latent heat of evaporation (J/kg)
T_W = Water temperature (°C)

6.4 Dynamic viscosity (μ)

$$\mu \approx 10^{-3} \times \exp\left[-3.7188 + \frac{578.919}{T_W + 135.604}\right] \tag{6.4}$$

where

μ = Dynamic viscosity of water (Pa-s)
T_W = Water temperature (°C)

Part III
Guide

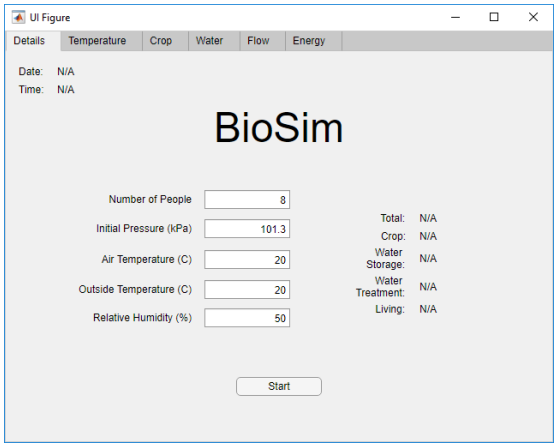

Figure 10: Start Page

To begin, BioSim requires a few initial parameters (Figure 10). These parameters determine the required area for crop growth, water treatment, and living space. They also set parameters about the environment which will change how energy, water and air move throughout the system.

Figure 11: Time step buttons

After clicking "Start", buttons will activate in the remaining tabs (Figure 11) which allow you to step the simulation for various time steps. A timer will also start in the upper left-hand corner which shows the current date and time.

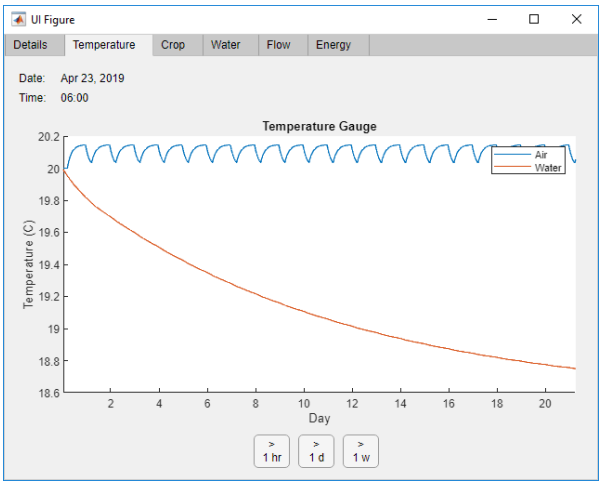

Figure 12: Temperature Page

The Temperature tab (Figure 12) shows the temperature of the air and water storage over time.

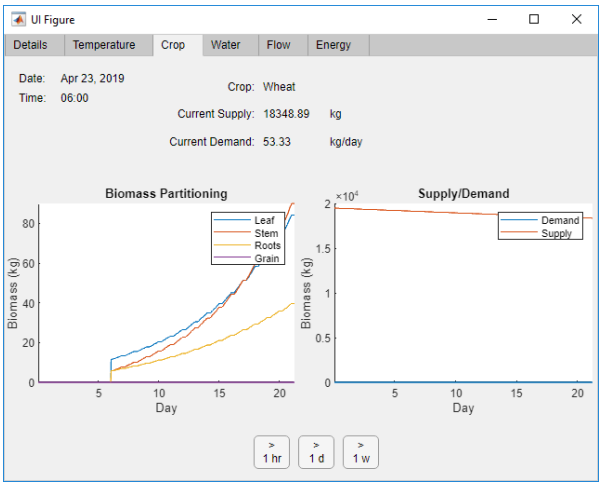

Figure 13: Crop Page

The Crop tab (Figure 13) shows the crop being grown, the amount in available supply, and the current demand. The graphs show the change in these values over time and how crop biomass partitions in the plants between leaves, stems, roots, and storage organs (grain).

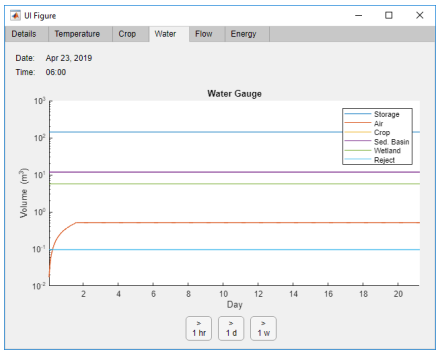

(a) Water Page

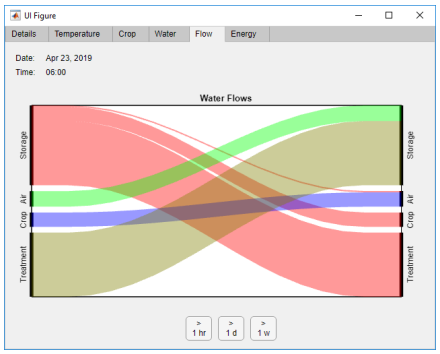

(b) Flows Page

The Water tab (Figure 14a) shows the distribution of water in the system. As everything is completely recycled, there is no net change in the total amount of water, only movement between different parts of the system. For this reason, the Flow tab (Figure 14b) shows the movement of water for the current hour.

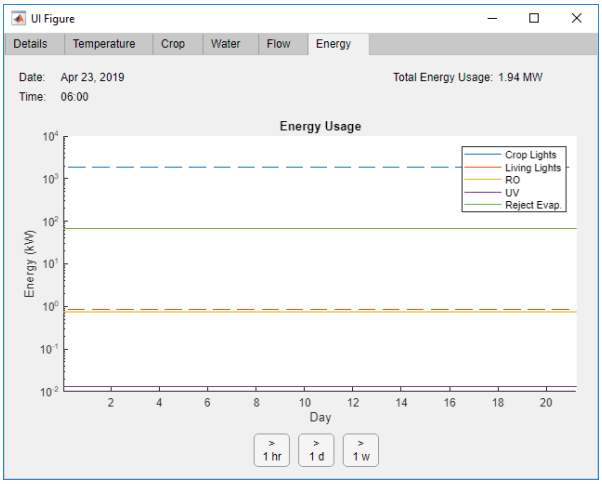

Figure 15: Energy Page

Finally, the Energy tab (Figure 15) shows the amount of energy consumption in different parts of the system on a logarithmic scale.

Part IV
Results & Discussion

7 Results

For the default initial parameters[10], the results for crop production and energy consumption are shown below (Figures 16a and 16b).

Crop production was cyclical at roughly 90 days between harvests. The area required for crop growth was 106 m^2/person and an initial supply of 54 kg/person of grain was needed to meet demand until the first harvest.

Energy usage for BioSim was distributed mainly to crop growth (lighting), which accounted for 79.6% of total energy usage during daylight hours, while the next highest energy user was evaporation of concentrated RO brine (19.7%). The remaining energy demands (living area lighting, RO pump, and UV disinfection) contributed only 0.70% of daylight energy requirements.

Treatment of wastewater was accomplished with minimal energy and area requirements. Total treatment area accounted for less than 2% of total area with the constructed wetlands requiring the most area (2.1 m^2/person). The sedimentation basin was used to remove particles over 100 μm while the constructed wetland removed nearly 100% of remaining TSS using a 70 mm day^{-1} loading rate. Further, head loss in the wetland was found to be near 0 using the Ergun equation.

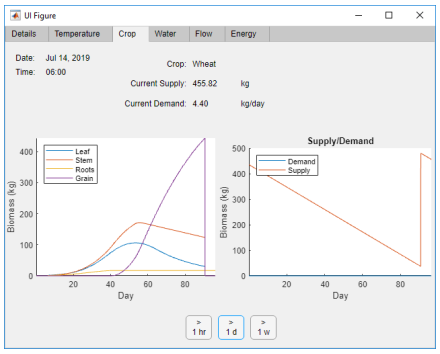

(a) Crop Growth results

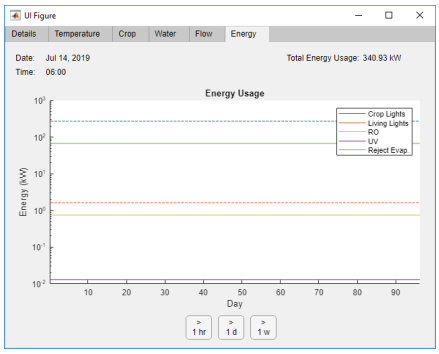

(b) Energy Consumption results

[10] 8 people, sea level pressure, 50% humidity, $T_a = T_o = 20°C$

8 Discussion

While the results provide a meaningful glimpse into the construction of such an environment, there are many questions which remain unanswered due to the difficulty in modeling many of these systems, and a larger question of what good a model of this nature could serve in a real-world situation.

Regarding the first set of questions, the crop growth system stands out as a difficult system to model. The equations which govern crop development and partitioning of biomass are dependent on several factors and while there are many rigorous models, the model chosen, albeit simple, requires a number of empirical parameters. Empirical data used in this study came from the investigation of rice crops in Asia [35] and it is reasonable to wonder if there is enough parallel between rice and wheat crops that the parameters controlling the partitioning of biomass in one can be used in the other. It would be interesting to compare these results to those of a more complete model such as CERES-Wheat, part of DSSAT (`https://apps.agapps.org/ide/serial/`), which was used in Biosphere 2 to model wheat growth to within 10% accuracy [31].

There is also a question regarding the completeness of a diet which is 100% wheat. The crop was chosen because of the ease of access to relevant information and was only configured to provide the required 2000 calories per day. But there are several limitations in consuming just one crop and especially one that is not so nutritionally robust. Ideally, as was done in Biosphere 2, multiple crops of different varieties and nutritional compositions were grown which provided the required calories as well as vitamins and minerals, with supplements integrated as needed [21].

Another variable which could use further exploration is the area configured for crop growth. Currently, the area is configured to minimize the amount of storage necessary. In a real-life situation, there would be a trade-off between storage of the crop and the amount of area dedicated to growing crops. Alternative means of food production should thus be explored as well. Other techniques, such as hydroponics or aquaponics, may provide a reduction in the amount of space required without sacrificing total crop/calorie production. In the case of aquaponics, which is a hydroponics system combined with an aquaculture system, an additional source of protein can be grown alongside crops which is otherwise difficult to find in plant-based sources.

Biosphere 2's agriculture module provided 7 people a year-round nutritionally dense diet with about 2000 m^3 of area and hosted a diverse ecology of insects and animals [18]. If a human habitat were to be constructed on Mars, a bigger discussion over the cost and feasibility of such a large area per person would need to take place since the resources necessary to build it will either need to be made on Mars or shipped from Earth. Concrete, for example, can likely be redesigned for Mars's unique soil chemistry and not have to be transported from Earth [34], however the same soil will require fertilizers in order to grow crops [13].

Carbon and nitrogen cycles were not modeled in this experiment. One of the larger issues in real-life experiments of this type, like Biosphere 2, was controlling

high CO_2 and maintaining adequate oxygen levels. The authors state:

> The studies revealed that the agricultural biome was the greatest contributor of CO_2, due to carbon rich soil, to the atmosphere and the greatest consumer of atmospheric O_2, which was then locked up primarily in the massive concrete structural elements of the facility. This one way flow of O_2 bound by CO_2 into the concrete as carbonates and the low leak rates, resulted in a potentially life-threatening circumstance for the Biospherians that ultimately required the injection of O_2 [17].

A fully-developed extension of BioSim would likely be necessary in predicting many of these factors and determining feasibility and cost estimates. Projects like Bios-3 and Biosphere 2 uncovered some surprising aspects of these constructed environments and contributed to the list of questions which must be answered before settling on the Moon or Mars. Still, it seems, there is a lot of work that remains before an extraterrestrial human settlement is a foregone conclusion.

Part V
Appendices

A Software Listing

The code for the model can be found online at `https://github.com/dnys1/biosim`.

References

[1] John Allen and Mark Nelson. "Overview and Design Biospherics and Biosphere 2, mission one (1991–1993)". In: *Ecological Engineering* 13.1 (June 1999), pp. 15–29. ISSN: 0925-8574. DOI: 10.1016/S0925-8574(98)00089-5.

[2] M. Bahrami. *Forced Convection Heat Transfer*.

[3] John Billingham et al. *Space Resources and Space Settlements*. SP-428. 1979, p. 300. URL: http://hdl.handle.net/2060/19790024054.

[4] Kim Binstead and Bryan Caldwell. "HI-SEAS Media Kit". In: (Jan. 2018). URL: http://hi-seas.org/?cat=103.

[5] Steven C. Chapra. *Surface water-quality modeling*. McGraw-Hill series in water resources and environmental engineering. New York: McGraw-Hill, 1997. ISBN: 978-0-07-011364-0.

[6] Maria Manuela Cruz-Cunha et al. "A Multiplayer Team Performance Task: Design and Evaluation". In: *Business, Technological, and Social Dimensions of Computer Games: Multidisciplinary Developments*. IGI Global, 2011, pp. 201–219.

[7] William F Dempster. "Biosphere 2 engineering design". In: *Ecological Engineering* 13.1 (June 1999), pp. 31–42. ISSN: 0925-8574. DOI: 10.1016/S0925-8574(98)00090-1.

[8] William F. Dempster. "Biosphere 2: System dynamics and observations during the initial two-year closure". In: Society of Automotive Engineers, July 1993.

[9] William F. Dempster. "Methods for measurement and control of leakage in CELSS and their application and performance in the biosphere 2 facility". In: *Advances in Space Research* 14.11 (Nov. 1994), pp. 331–335. ISSN: 02731177. DOI: 10.1016/0273-1177(94)90318-2.

[10] Margaret Garcia. *Lecture 7*.

[11] J.L. Garland et al. "Integration of waste processing and biomass production systems as part of the KSC Breadboard project". In: *Advances in Space Research* 20.10 (Jan. 1997), pp. 1821–1826. ISSN: 02731177. DOI: 10.1016/S0273-1177(97)00847-8.

[12] Kerry J. Howe et al. *Principles of water treatment*. Ed. by MWH Americas Staff. Wiley, 2012. URL: https://ebookcentral-proquest-com.ezproxy1.lib.asu.edu/lib/asulib-ebooks/detail.action?docID=947864.

[13] Gary Jordan. *Can Plants Grow with Mars Soil?* Aug. 2017. URL: https://www.nasa.gov/feature/can-plants-grow-with-mars-soil.

[14] Robert H. Kadlec, Scott Wallace, and Robert L. Knight. *Treatment Wetlands: Theory and Implementation*. CRC Press, 2008. URL: https://ebookcentral-proquest-com.ezproxy1.lib.asu.edu/lib/asulib-ebooks/detail.action?docID=360079.

[15] Cindy S. Kao and James R. Hunt. "Prediction of wetting front movement during one-dimensional infiltration into soils". In: *Water Resources Research* 32.1 (Jan. 1996), pp. 55–64. DOI: 10.1029/95WR02974. URL: https://agupubs.onlinelibrary.wiley.com/doi/pdf/10.1029/95WR02974.

[16] W. M. Knott. "The breadboard project: A functioning CELSS plant growth system". In: *Advances in Space Research* 12.5 (Jan. 1992), pp. 45–52. ISSN: 02731177. DOI: 10.1016/0273-1177(92)90009-M.

[17] Bruno D.V. Marino and H.T. Odum. "Biosphere 2: Introduction and research progress". In: *Ecological Engineering* 13.1 (June 1999), pp. 3–14. ISSN: 0925-8574. DOI: 10.1016/S0925-8574(98)00088-3.

[18] Bruno D.V. Marino et al. "The agricultural biome of Biosphere 2:: Structure, composition and function". In: *Ecological Engineering* 13.1 (June 1999), pp. 199–234. ISSN: 0925-8574. DOI: 10.1016/S0925-8574(98)00100-1.

[19] Víctor Matamoros et al. "Removal of Pharmaceuticals and Personal Care Products (PPCPs) from Urban Wastewater in a Pilot Vertical Flow Constructed Wetland and a Sand Filter". In: *Environmental Science & Technology* 41.23 (2007). PMID: 18186355, pp. 8171–8177. DOI: 10.1021/es071594+. eprint: https://doi.org/10.1021/es071594+. URL: https://doi.org/10.1021/es071594+.

[20] Institute of Medicine. *Review of NASA's Human Research Program Evidence Books: A Letter Report*. Washington, DC: The National Academies Press, 2008. DOI: 10.17226/12261. URL: https://www.nap.edu/catalog/12261/review-of-nasas-human-research-program-evidence-books-a-letter.

[21] Dennis Mock et al. "Calorie Restriction in Biosphere 2: Alterations in Physiologic, Hematologic, Hormonal, and Biochemical Parameters in Humans Restricted for a 2-Year Period". In: *The Journals of Gerontology: Series A* 57.6 (June 2002), B211–B224. ISSN: 1079-5006. DOI: 10.1093/gerona/57.6.B211. eprint: http://oup.prod.sis.lan/biomedgerontology/article-pdf/57/6/B211/9732904/B211.pdf. URL: https://doi.org/10.1093/gerona/57.6.B211.

[22] NASA. *Human Research Roadmap - Introduction*. URL: https://humanresearchroadmap.nasa.gov/intro/.

[23] Mark Nelson et al. "Bioregenerative recycling of wastewater in Biosphere 2 using a constructed wetland: 2-year results". In: *Ecological Engineering* 13.1 (June 1999), pp. 189–197. ISSN: 0925-8574. DOI: 10.1016/S0925-8574(98)00099-8.

[24] NMSU. *New Mexico Irrigation Center*. URL: https://aces.nmsu.edu/aes/irrigation/.

[25] F. Penning de Vries F. W. T and H. H. van. Laar. *Simulation of plant growth and crop production*. Centre for Agricultural Publishing Documentation, 1982.

[26] Janet V. Powers. *Publications of the NASA Controlled Ecological Life Support System (CELSS) Program 1989-1992*. 4603. 1994. URL: http://hdl.handle.net/2060/19940025617.

[27] Frank B. Salisbury, Josef I. Gitelson, and Genry M. Lisovsky. "Bios-3: Siberian Experiments in Bioregenerative Life Support". In: *BioScience* 47.9 (Oct. 1997), pp. 575–585. ISSN: 00063568, 15253244. DOI: 10.2307/1313164.

[28] Serge Savary and Laetitia Willocquet. "Crop Growth Modeling - Introducing GENECROP as a Framework". In: *The Plant Health Instructor* (2014). DOI: 10.1094/PHI-A-2014-0314-01. URL: https://www.apsnet.org/edcenter/advanced/topics/BotanicalEpidemiology/Pages/CropGrowthModeling.aspx.

[29] Jeffrey P. Severinghaus et al. "Oxygen loss in biosphere 2". In: *Eos, Transactions American Geophysical Union* 75.3 (1994), pp. 33, 35–37. ISSN: 0096-3941. DOI: 10.1029/94EO00285.

[30] Scott M. Smith, Sara R. Zwart, and Martina Heer. *Evidence Report: Risk Factor of Inadequate Nutrition*. Human Research Program. Jan. 2015.

[31] Francesco N Tubiello et al. "Growing wheat in Biosphere 2 under elevated CO2: Observations and modeling". In: *Ecological Engineering* 13.1 (June 1999), pp. 273–286. ISSN: 0925-8574. DOI: 10.1016/S0925-8574(98)00104-9.

[32] Janice S. Wallace and Janet V. Powers. *Publications of the NASA Controlled Ecological Life Support System (CELSS) Program, 1979-1989*. 4297. 1990. URL: http://hdl.handle.net/2060/19900012438.

[33] E. Walters et al. "Influence of Particle Association and Suspended Solids on UV Inactivation of Fecal Indicator Bacteria in an Urban River". In: *Water, Air, & Soil Pollution* 225.1 (Dec. 2013), p. 1822. ISSN: 1573-2932. DOI: 10.1007/s11270-013-1822-8. URL: https://doi.org/10.1007/s11270-013-1822-8.

[34] Lin Wan, Roman Wendner, and Gianluca Cusatis. "A novel material for in situ construction on Mars: experiments and numerical simulations". In: *Construction and Building Materials* 120 (2016), pp. 222–231. ISSN: 0950-0618. DOI: https://doi.org/10.1016/j.conbuildmat.2016.05.046. URL: http://www.sciencedirect.com/science/article/pii/S095006181630770X.

[35] L Willocquet et al. "Structure and validation of RICEPEST, a production situation-driven, crop growth model simulating rice yield response to multiple pest injuries for tropical Asia". In: *Ecological Modelling* 153.3 (2002), pp. 247–268. ISSN: 0304-3800. DOI: https://doi.org/10.1016/S0304-3800(02)00014-5. URL: http://www.sciencedirect.com/science/article/pii/S0304380002000145.

[36] Bernd Zabel et al. "Construction and engineering of a created environment: Overview of the Biosphere 2 closed system". In: *Ecological Engineering* 13.1 (June 1999), pp. 43–63. ISSN: 0925-8574. DOI: 10.1016/S0925-8574(98)00091-3.

[37] Lincoln Zotarelli et al. *Step by Step Calculation of the Penman-Monteith Evapotranspiration (FAO-56 Method)*. Tech. rep. AE459. University of Florida, IFAS Extension, 2015.